RESEARCH INVESTIGATION OF LASER LINE PROFILES

REPORT F920479-6
SEMI-ANNUAL REPORT

PERIOD COVERED: 1 AUGUST 1967 TO 31 JANUARY 1968

PREPARED UNDER CONTRACT NO(14-66-C0344
ARPA ORDER NO. 306, PROJECT COST CODE NO. 6E30K21

United Aircraft Research Laboratories
UNITED AIRCRAFT CORPORATION
EAST HARTFORD, CONNECTICUT

UNITED AIRCRAFT CORPORATION
RESEARCH LABORATORIES
East Hartford, Connecticut

F-920479-6
Semiannual Report Under
Contract N00014-66-C0344
1 August 1967
through
31 January 1968

Project Title: RESEARCH INVESTIGATION OF LASER LINE PROFILES
Name of Contractor: United Aircraft Corporation Research Laboratories
Project Code No. 6E30K21
ARPA Order No. 306

This research is part of Project DEFENDER under the joint sponsorship of the Advanced Research Projects Agency, the Office of Naval Research, and the Department of Defense.

Reported By:

M. J. Brienza
Chief, Applied Laser Technology

A. J. DeMaria
Senior Principal Scientist
Quantum Physics Laboratory

W. H. Glenn, Jr.
Principal Scientist,
Quantum Physics

G. L. Lamb, Jr.
Senior Theoretical Physicist

M. E. Mack
Research Scientist

E. B. Treacy
Senior Research Scientist

Approved By:

A. J. DeMaria
Senior Principal Scientist
Quantum Physics Laboratory

Date: February 28, 1968

Report F-920479-6

Semiannual Report Under Contract N00014-66-C0344
for the Period 1 August 1967 through 31 January 1968

RESEARCH INVESTIGATION OF LASER LINE PROFILES

ARPA Order No. 306, Project Code No. 6E30K21

TABLE OF CONTENTS

Report F-920479-6

Semiannual Report under Contract N00014-66-C0344
for the Period 1 August 1967 through 31 January 1968

Research Investigation of Laser Line Profiles

ARPA Order No. 306, Project Code No. 6E30K21

SUMMARY

This report presents a summary of the research performed by the Research Laboratories of United Aircraft Corporation during the six-month interval from 1 August 1967 to 31 January 1968 on research directed toward advancing the state of the art of ultrashort laser pulse technology. This effort has resulted in the following enhancement of the ultrashort laser pulse technology field:

(a) Mode-Locking of an Organic Dye Laser. This accomplishment should make available picosecond optical pulses throughout the visible portion of the spectrum. The availability of ultrashort pulses at any desired wavelength would greatly increase their applicability to studies of nonlinear optical effects, spectroscopy, lifetime measurements, etc.

(b) Optical Rectification of Mode-Locked Laser Pulses at Microwave Frequencies. This accomplishment opens up the possibility of generating millimeter or submillimeter waves with ultrashort optical pulses and obtaining a detector for picosecond pulses because of the broad band response of the optical rectification effect. The detection of optical rectification at approximately 10 GHz has eliminated spurious signals from pyroelectric and acoustic effects therefore simplifying the detection of this effect. The use of simultaneously Q-switched and mode-locked pulses enables the use of the high sensitivity characteristics of radio receivers in many experiments where signal sensitivity may be a problem.

(c) Analytical Solution for 2π and 4π Optical Pulses. This accomplishment should lead to a better understanding of the transient response of quantum systems.

(d) Theoretical Prediction of Adiabatic Inversion of Quantum States. This accomplishment should result in a better understanding of the transient response of quantum systems when subjected to a frequency-swept laser pulse.

(e) 60 MHz Frequency-Swept, Q-Switched CO_2 Laser Pulse. This accomplishment should open up new experimental possibilities in studying transient response of quantum systems and in optical ranging, radar, signal processing, etc.

(f) Measurement of Nanosecond Fluorescence Decay Times. This accomplishment has demonstrated the ease at which subnanosecond fluorescence lifetime can be measured with ultrashort laser pulses having peak powers of the order of gigawatts. This technique should therefore be of great help to spectroscopists in their study of solids, liquids, and gases.

(g) Light Amplification in Saturable Absorbers (LAISA) with Picosecond Pulses. This accomplishment has resulted in a new method for amplifying light waves and therefore suggests that the device be called a "LAISA", an acronym for "Light Amplification in Saturable Absorbers."

INTRODUCTION

Q-switched laser pulses have found wide usage in studying gas breakdown at optical frequencies, thermonuclear research, optical harmonic generation, stimulated Raman and Brillouin scattering effects, photon echoes, surface emission effects, self-induced optical transparency, stimulated four-photon scattering, etc. These pulses have also found wide military usage in semiactive guidance, ranging, high-speed photography, radiation weapon research, etc. The minimum pulse widths obtainable with the various existing Q-switching techniques are limited to approximately 10^{-8} sec because of the requirement of one or more passes through the laser medium to build up the laser pulse. Numerous applications of single and multiple high-peak power laser pulses of time duration of 10^{-9} to 10^{-13} sec in the aforementioned areas of military and industrial research and applications are potentially very attractive. For example, the use of an optical pulse of 10^{-10} sec time duration would enable the measurement of distances of miles to an accuracy of a few cm. The use of pulses of 10^{-9} to 10^{-13} sec time duration and of gigawatts of peak power in nonlinear optics and transient response of quantum systems research is promising. The interaction of high-peak power coherent radiation of short time duration with both organic and inorganic matter is of great interest to academic, military, and industrial researchers.

During the last two years the Research Laboratories of United Aircraft Corporation have been conducting both inhouse and government sponsored programs which have resulted in techniques for generating and measuring laser pulses of 4×10^{-12} sec with Nd^{3+}:glass and of 10×10^{-12} sec with ruby lasers. Data indicates that a lower limit of 2×10^{-13} sec exists for such pulse generation techniques with Nd:glass lasers. With one stage of amplification, peak powers of 10^{+11} watts have been obtained. Electrical pulses of 90×10^{-12} sec risetime, 65 volts peak, and up to 2 nanosecond repetition rate have been obtained with stimultaneous Q-switched and mode-locked Nd^{3+}:doped glass oscillators and fast photodiode detector combinations. Electrical pulses with these characteristics were previously unavailable with conventional electronic devices. The generation of these electrical pulses by high-peak power, mode-locked lasers would also be of interest to the electronic industry for the determination of the location and severity of internal reflections in wide-bandwidth transmission systems, propagation delay studies, bandwidth measurements, etc. Ultrashort laser pulses have also been utilized at the Research Laboratories of United Aircraft Corporation to: (a) generate ultrashort acoustic pulses having harmonic contents up to 3.1 GHz, (b) measure nanosecond lifetimes of Q-switching dye solutions, (c) observe optical rectification up to 10 GHz, (d) generate ultrashort optical pulses at various wavelengths in the visible region with laser pumped dye lasers, and (e) observe "Light Amplification in Saturable Absorbers" (LAISA) with picosecond pulses.

MODE-LOCKING OF AN ORGANIC DYE LASER

It has been reported that a large number of organic dye solutions exhibit laser action when excited with a short duration, high-intensity pump pulse (Refs. 1-5). Pump pulses from Q-switched lasers and from specially constructed flash tubes have been employed. The output spectra from such dye lasers are quite broad, extending in some cases over a few hundred angstroms. This suggests the possibility of mode-locking an organic dye laser to produce very short (picosecond or shorter) pulses over a wide range of the visible spectrum. The availability of ultrashort pulses with any desired wavelength would greatly increase their applicability to studies of nonlinear transient optical effects, spectroscopy, and lifetime measurements (Ref. 6).

Research conducted under this contract has resulted in the mode-locking of a dye laser by pumping with another mode-locked laser. It is well known that a periodic modulation of the gain of a laser medium will lead to mode-locking if the frequency of the modulation is equal to or a multiple of the difference frequency between longitudinal modes of the laser.

If the pumping signal for a dye laser consists of a mode-locked train of pulses, the gain of the laser will have a periodic variation with a period equal to the spacing between the pumping pulses. If the length of the dye laser cavity is equal to or a submultiple of the length of the cavity of the laser producing the pump pulses, then the mode-locking condition will be satisfied and the output of the dye laser will consist of a series of pulses.

In the present experiment two dyes were used, Rhodamine 6G and Rhodamine B. These dyes, in ethanol solution, have absorption peaks at 5260 Å and 5500 Å. The peaks are sufficiently broad to allow efficient pumping with the 5300 Å second harmonic of the Nd-laser. The dye laser was constructed as shown in Fig. 1. The cell was 2.5 cm in diameter and 5 cm in length. The windows were optically flat and positioned almost perpendicular to the axis of the cell. The mirrors had a 1-meter radius of curvature and a reflectivity in excess of 90% between 5000 Å and 6000 Å. The second harmonic required for pumping was generated in the dye cavity with a crystal of phase-matched KDP. The efficiency of conversion of the 1.06-micron radiation to second harmonic was measured to be approximately 2%. A slight focusing of the fundamental radiation into the dye laser cavity was required to reach threshold.

The strength of the dye solution was adjusted by gradually increasing the dye concentration until the second harmonic radiation was almost completely absorbed in the cell. Typical concentrations used were about 5×10^{-5} molar.

The pump signal was generated as the second harmonic from a Nd-glass laser that was mode-locked with Eastman Kodak 9740 dye (Refs. 6 and 7). The length of the rod was 6" and the diameter 0.5". The output consisted of a train of subnanosecond pulses spaced by approximately 5×10^{-9} sec and lasted approximately 2×10^{-7} sec.

Lasing was observed with the optical length of the dye laser cavity equal to 1, 1/2 and 1/3 times the length of the pumping laser cavity. Figure 2a shows a typical output of the pumping laser. Figure 2b shows a synchronous trace of the dye laser output. In this case the dye laser cavity was adjusted to be one-half of the length of the pumping laser cavity. The dye used in this case was Rhodamine 6G in ethanol. The dye laser output shows very small fluorescence until the pumping signal reaches threshold, at which point the dye laser breaks into oscillation and produces a series of pulses at twice the repetition rate of the pumping pulses. The energy scale on the traces is intended to give a rough estimate of the pulse energies. The vertical axis is given in energy rather than power because the fundamental pulses are shorter than the response time of the detector. The pulse shape is thus characteristic of the detector rather than any property of the pulse. The only quantity that can be measured is the total energy of the pulse, which is proportional to the amplitude of the detector-limited pulse shape. The same procedure was used for the dye laser output, with appropriate scaling of the spectral sensitivities of the two diodes. These values are somewhat uncertain, therefore, since the pulse duration is comparable to the detector response time.

Figures 2c, 2d show the spectral output of the dye laser and a mercury reference spectrum. Figure 2c shows the output for a 5×10^{-5} molar solution of Rhodamine B in ethanol. The output occurs slightly above the 5790 Å line of the mercury spectrum. For Rhodamine 6G of comparable concentration, the line appears midway between the two mercury lines, at 5600 Å. If Rhodamine 6G is added to the Rhodamine B solution, the line moves continuously from one limit to the other. Such an intermediate case is shown in Fig. 2d.

It was noted that the spectral width of the output of the laser was not as great as has been reported (Ref. 1). It is believed that this is due to the fact that the laser was operating just above threshold. Sufficient pump power was not available in these initial experiments to operate the laser far enough above threshold to give a wider spectral output. The output pulses from the laser were also broader than those of the pump. This is a result of the fact that the laser operates only during a fraction of the pumping time and there is insufficient time to allow the locking of all the modes. Higher pumping power should eliminate both of these problems and allow the generation of picosecond pulses throughout the visible spectrum.

OPTICAL RECTIFICATION OF MODE-LOCKED LASER PULSES

The optical rectification (i.e., the nonlinear optical dc polarization) effect was first observed by Bass, et al, in the form of an induced dc voltage across a crystal of potassium dihydrogen phosphate (KDP) during the passage of an intense ruby laser pulse through the crystal (Ref. 8). Considerable difficulty is normally encountered in experimentally observing optical rectification because of the low voltage signals generated by the effect, the requirement of relatively broad band and thus insensitive electronic equipment, electrical noise arising from the flash lamp trigger and discharge, and spurious signals due to pyroelectric (Ref. 8) and acoustic waves generated by the optical electrostriction and transient heating effects (Ref. 9).

The purpose of this Letter is to report the observation of harmonically-rich electrical pulses generated in crystals of lithium niobate and KDP by the optical rectification of the output of a simultaneously Q-switched and mode-locked Nd:glass laser (Ref. 6). The periodic pulsating characteristics of such lasers enabled us to make use of the high sensitivity and selectivity of radio receivers in detecting the effect. The large signal-to-noise ratio obtained by use of a mode-locked laser and a radio receiver in the experiments enabled us to easily identify (and thus eliminate) spurious acoustic signals by their repetitive echo characteristics. In addition, signals from relatively slow effects such as the pyroelectric effect were eliminated by detecting the harmonics of the optical rectification signals in the microwave region.

The output of the mode-locked Nd:glass laser used in our experiments consisted of a series of light pulses of 10^{-12} to 10^{-11} sec time duration (Refs. 6, 10, 11), evenly spaced by the optical transit time of the laser cavity. The fundamental frequency of the pulse train used here was 275 MHz. The average energy in the individual pulses was typically of the order of 1 mJ. The entire pulse train contained approximately 200 pulses and lasted about 0.6μ sec. The laser output was directed through crystals of lithium niobate and KDP either along or perpendicular to the z-axis of the crystals. A flat-ended coaxial probe fixed against the surface normal to the z-axis was used to sense the induced fields present at that surface. A 5-mil-thick annular mylar gasket was used to prevent an intimate contact between the center probe and the crystal surface to eliminate the possible acoustic effects (Ref. 9) which might cause spurious signals through the surface piezoelectric effect, especially in the case of lithium niobate. Such acoustic signals could be identified by their repetitive echo characteristics. The rf signals were measured to be approximately 2 mv and were detected by a superheterodyne receiver having a 20 MHz bandwidth.

The observed signals were recorded with a signal-to-noise ratio of up to 20 to 25 db and followed the general features of the envelope of the laser pulse train which was simultaneously recorded. Signals were recorded at each harmonic frequency from 275 MHz to 9.025 GHz and were limited only by the available equipment. As

evidenced by tuning the radio receiver, the signals were as well confined to the harmonic frequencies of the laser pulse repetition frequency as the bandwidth of the receiver could determine. The actual bandwidth of the observed signals can be calculated from the length of the entire pulse train. In the case of lithium niobate the phase matching angle for efficient second harmonic light production is very nearly normal to the optic axis so it was possible to simultaneously observe the optical rectification signal, the second harmonic (green) light output and the original input laser pulse train.

Figure 3 schematically illustrates the orientation of the crystallographic axes of KDP with respect to the polarization of the repetitive pulses. For KDP illuminated along the z-axis, the dc part of the polarization reduces simply to $P_z = 1/2 X_{zxy} E_x E_y$, where X_{zxy} is the third rank nonlinear dielectric tensor for KDP. If α is the angle between the plane of polarization of the laser light and the x-axis of the KDP, P_z will vary as $\sin 2\alpha$. Figure 4 shows the relative strength of the rf signals at 2.75 GHz recorded as a function of α. The $\sin 2\alpha$ function has been normalized and drawn as the dashed curve for comparison. Similar data were observed at other harmonic frequencies. Signals from relatively slow effects, such as the pyroelectric effect, were eliminated by detecting the optical rectification effect at microwave frequencies. Figure 5 illustrates typical oscillograms of the optical rectification and laser output signals.

The broad band response of the optical rectification effect, coupled with greatly increased sensitivity obtained with radio receivers and repetitive picosecond laser pulses, suggests the use of the effect for detecting picosecond light pulses and for generating millimeter and submillimeter radiation. Optical pulse measurement by the optical rectification effect is similar to pulse intensity correlation measurements (Refs. 10-12). The correlation measurements reported in the past were performed in the Fourier transform or frequency domain. Some unique characteristics of such a microwave generating system would be its broad band passive generating element (i.e., the nonlinear crystal) whose operating frequencies can be easily changed and precisely specified by adjustment of the laser cavity length. The upper operating frequency of the device is limited only by the harmonic content of the available ultrashort laser pulses.

PROPAGATION CHARACTERISTICS OF ULTRASHORT OPTICAL PULSES

Optical pulses of 10^{-12} sec duration have recently been produced (Refs. 7, 3, 10, 11) by the simultaneous Q-switching and mode-locking of Nd^{3+}:glass lasers. Such pulse widths are comparable to the transverse relaxation time of the medium. Pulses shorter than the transverse relaxation time may be obtained by additional experimental modifications (low temperatures). The simplicity of the theoretical model which describes this situation provides considerable insight into many features of optical pulse propagation in an active medium. The self-induced transparency effect recently discussed by McCall and Hahn (Ref. 14) and the pulse

splitting obtained from machine computation by the same authors and observed by Patel and Slusher (Ref. 15) may be exhibited within a completely analytic framework of this model.

When the pulse length is short compared to the longitudinal and transverse relaxation times of the medium, the electric field of the optical pulse $E(x,t)$, the macroscopic polarization density of the medium $P(x,t)$ and the population inversion $N(x,t)$ are related through the equations (Ref. 16).

$$\frac{\partial^2 E}{\partial x^2} - \frac{1}{c^2}\frac{\partial^2 E}{\partial t^2} = \frac{4\pi}{c^2}\frac{\partial^2 P}{\partial t^2}, \tag{1}$$

$$\frac{\partial^2 P}{\partial t^2} + \omega^2 P = -\frac{\omega}{\hbar}\wp^2 EN, \tag{2}$$

$$\frac{\partial N}{\partial t} = -\frac{2}{\hbar\omega} E\frac{\partial P}{\partial t}, \tag{3}$$

where E_o is the transition frequency of the two-level systems and N_o is the dipole matrix element connecting the two energy levels. It will be assumed that all two-level systems have exactly the same transition frequency and that the carrier frequency of the light pulse is at this same frequency. The necessary bandwidth of the medium required to transmit the pulse is provided by a saturation broadening effect.

Since even the shortest pulses produced to date contain many optical cycles, it is appropriate to introduce the assumption that E and P are of the form

$$E(x,t) = \mathcal{E}_o \mathcal{E}(x,t)\cos(kx - \omega t), \tag{4}$$

$$P(x,t) = N_o \wp \mathcal{P}(x,t)\sin(kx - \omega t), \tag{5}$$

where E_o is a characteristic field strength and N_o is the initial number density of active atoms in the upper state minus those in the lower state. The envelopes $\mathcal{E}(x,t)$ and $\mathcal{P}(x,t)$ have spatial and temporal variations which are slow compared to those of the optical carrier wave. The assumption of slow variation of $\mathcal{E}$ and $\mathcal{P}$ justifies the neglect of second derivatives and products of first derivatives when Eqs. (4) and (5) are substituted into Eqs. (1)-(3).

With this simplification, the equations relating $\mathcal{E}$, $\mathcal{P}$ and $\eta = N/N_o$ may be written in the dimensionless form

$$\frac{\partial \mathcal{E}}{\partial \xi} = \mathcal{P}, \tag{6}$$

$$\frac{\partial \rho}{\partial \tau} = \eta \mathcal{E} \tag{7}$$

$$\frac{\partial \eta}{\partial \tau} = -\mathcal{E} \rho . \tag{8}$$

The dimensionless variables are

$$\mathcal{E} = (\delta \Omega / c) x , \quad \tau = \Omega (t - x/c) , \tag{9}$$

where $\Omega = E_0 \theta / \hbar$ and $\delta = N_0 \hbar \omega / (E_0^2 / 2\pi)$. Energy conservation is readily exhibited by multiplying Eq. (6) by combining it with Eq. (8) and integrating overall terms. One finds

$$\frac{c E_0^2}{4\pi} \frac{\partial}{\partial x} \int_{-\infty}^{\infty} dt \mathcal{E}^2 (x,t) + N(x,\infty) \hbar \omega = N(x,-\infty) \hbar \omega . \tag{10}$$

Equations (7) and (8) admit of an immediate integral which may be expressed in the parametric form

$$N(\mathcal{E},\tau) = G(\mathcal{E}) \cos \sigma (\mathcal{E},\tau) , \tag{11}$$

$$\rho(\mathcal{E},\tau) = G(\mathcal{E}) \sin \sigma (\mathcal{E},\tau) , \tag{12}$$

where $\left[G(\mathcal{E})\right]^2 = \left[N(\mathcal{E},-\infty)\right]^2 + \left[\rho(\mathcal{E},-\infty)\right]^2$. Equation (7) yields

$$\mathcal{E} = \frac{\partial \sigma}{\partial \tau} , \tag{13}$$

and Eq. (6) then reduces to

$$\frac{\partial^2 \sigma}{\partial \mathcal{E} \partial \tau} = \sin \sigma . \tag{14}$$

Although the general solution of this equation is apparently unknown at present, considerable progress has been made in obtaining useful particular solutions by means of a Baecklund transformation (Ref. 17). Application of this transformation theory shows that two particular solutions of Eq. (14) are related by

$$\frac{1}{2} \frac{\partial}{\partial \tau} (\sigma_2 - \sigma_1) = \frac{1+\sin\theta}{\cos\theta} \sin \frac{1}{2} (\sigma_2 + \sigma_1) , \tag{15}$$

$$\frac{1}{2} \frac{\partial}{\partial \mathcal{E}} (\sigma_2 + \sigma_1) = \frac{1-\sin\theta}{\cos\theta} \sin \frac{1}{2} (\sigma_2 - \sigma_1) , \tag{16}$$

where θ is an arbitrary constant. Since $\sigma_1 = 0$ is a solution of Eq. (14), a second solution is readily obtained in the form

$$\sigma_2 = 4 \tan^{-1} \gamma \exp\left[\frac{\tau + \xi + (\tau - \xi)\sin\theta}{\cos\theta}\right], \tag{17}$$

where γ is an arbitrary constant. This solution has the property that as τ varies from $-\infty$ to $+\infty$, σ_2 varies from 0 to 2π. The corresponding variation in the population difference and polarization density may be immediately inferred from Eqs. (11) and (13). From Eq. (13) the normalized pulse shape is found to be

$$\mathcal{E}(x,t) = \operatorname{sech}(\Omega/2)(t - x/v), \tag{18}$$

where

$$\frac{1}{v} = \frac{1}{c}(1 - 4\delta). \tag{19}$$

This solution represents a pulse shape which propagates without distortion through a medium in which all atoms are initially in the upper state. The front portion of the pulse is continually amplified while the back is continually attenuated in such a way that the profile of the pulse moves through the medium faster than the light velocity. A similar result has also been obtained and observed experimentally by Basov, et al (Ref. 16).

More interesting features of pulse propagation are described by employing another result of the Baecklund transformation theory, namely that four solutions of Eq. (15) are related through

$$\tan\left(\frac{\sigma_3 - \sigma_0}{4}\right) = \frac{\cos 1/2(\theta_1 + \theta_2)}{\sin 1/2(\theta_1 - \theta_2)} \tan\left(\frac{\sigma_1 - \sigma_2}{4}\right), \tag{20}$$

In particular, the distortion of a pulse of sufficient strength to induce two inversions in the population of the active medium is described by using Eq. (20) with

$$\sigma_0 = 0, \tag{21}$$

$$\sigma_i = 4 \tan^{-1}\left\{\gamma_i \exp\left[\frac{\tau + \xi + (\tau - \xi)\sin\theta_i}{\cos\theta_i}\right]\right\}, \quad i = 1,2 . \tag{22}$$

Choosing $\theta_1 = \theta$, $\theta_2 = \pi$, $\gamma_1 = \gamma_2 = 1$, one finds

$$\sigma_3 = 4 \tan^{-1}\left[\tan\frac{\theta}{2} \frac{\sinh 1/2(\alpha + \beta)}{\cosh 1/2(\alpha - \beta)}\right], \tag{23}$$

where

$$\alpha = \frac{1+\sin\theta}{\cos\theta}\,\tau + \frac{1-\sin\theta}{\cos\theta}\,\xi \qquad (24)$$

$$\beta = \tau + \xi \,. \qquad (25)$$

As τ varies from $-\infty$ to $+\infty$, σ_3 varies from -2π to $+2\pi$. From Eq. (11) this variation in σ provides for two complete oscillations in an atomic population that is initially (and finally) in the upper state. The pulse shape is again obtained from Eq. (14) and one finds (Ref. 18)

$$\mathcal{E}(x,t) = \frac{2\sin\theta\left\{\operatorname{sech}\left[\Omega(t-x/v)\right] + a\operatorname{sech}\left[a\Omega(t-x/v')\right]\right\}}{1-\cos\theta\left\{\tanh\left[\Omega(t-x/v)\right]\tanh\left[a\Omega(t-x/v')\right] - \operatorname{sech}\left[\Omega(t-x/v)\right]\operatorname{sech}\left[a\Omega(t-x/v')\right]\right\}} \qquad (26)$$

where $a = (1+\sin\theta)/\cos\theta$, $v' = c/(1-\mathcal{E}/a^2)$ and v is given by Eq. (19). For $\mathcal{E}$ to be positive, one requires $0 < \theta < \pi/2$ from which it follows that a is greater than unity and, hence, $v' < v$. As this pulse propagates through the medium, it effectively splits into two separate pulses. The attenuation of the midportion of the pulse takes place because the active medium is predominantly in the lower level during the time that this portion of the pulse interacts with it.

Figure 6 illustrates a pulse shape predicted by Eq. (26) as a function of the retarded time $\tau = t - x/v$ for $\theta = \pi/3$, $\mathcal{E} = -1/2$. Direction of propagation is to the left in the figure. Figure 7 is a similar result for $\theta = \cos^{-1}(2/3)$, $\mathcal{E} = -1/2$.

From these figures it is clear that the leading pulse has an amplitude determined by the initial wave shape, while the second pulse is of the type obtained from Eq. (18).

INTERACTION OF INTENSE FREQUENCY-SWEPT LASER PULSES WITH MATTER

A theoretical investigation of the interaction of an intense frequency-swept pulse of light (i.e., an optical chirp) with matter has been conducted. The first interesting result to come out of the investigation was the adiabatic inversion of populations between a pair of levels when the frequency of the pulse is swept through their resonant frequency. The second result was the dependence of the phase of the induced polarization on the direction of the sweep. These effects have been observed in nuclear magnetic induction experiments (Ref. 19), and the new features in our experiments will be: (1) the use of electric dipole transitions, (2) excitation of the sample by a traveling wave. These are the two features that distinguish the so-called "photon" echo (Ref. 20) from the well-known spin echo

experiments (Refs. 21, 22). In addition, the frequency is swept across the otherwise unperturbed resonance between the levels in our experiments, whereas in NMR the frequency is held fixed and the energy level spacing is swept by the external magnetic field.

The geometrical representation of the Schrodinger equation due to Feyman, et al (Ref. 23) provides a lucid description of the phenomenon. The Schrodinger equation

$$i\hbar \frac{\partial \psi}{\partial t} = H\psi = H_o\psi + V\psi \tag{27a}$$

is rewritten

$$\frac{d\vec{r}}{dt} = \vec{\omega} \times \vec{r}, \tag{27b}$$

where

$$\psi(t) = a(t)\psi_a + b(t)\psi_b. \tag{28}$$

For $m = \pm 1$ transitions, the following relationships hold for the parameters of Eqs. (27) and (28):

$$\hbar\omega_1 = V_{ab} + V_{ba} = -\gamma E_x, \tag{29a}$$

$$\hbar\omega_2 = i(V_{ab} - V_{ba}) = -\gamma E_y, \tag{29b}$$

$$\hbar\omega_3 = \hbar\omega_o = E_b - E_a, \tag{29c}$$

$$r_1 = ab^* + a^*b, \tag{30a}$$

$$r_2 = i(ab^* - a^*b), \tag{30b}$$

$$r = a^*a - b^*b \tag{30c}$$

where $\gamma = \mu_{ab}^{+} = \mu_{ba}^{-}$ is the dipole moment operator. The precession of $\vec{r}$ about the resultant $\vec{\omega}$ is completely analogous to the precession of the nuclear moment $\vec{\mu}$ about a resultant magnetic field B.

For a pulse having the following electric field components

$$E_x = A(t)\cos\phi(t), \tag{31a}$$

$$E_y = A(t)\sin\phi(t), \tag{31b}$$

the picture is simplified by referring the vector $\vec{r}$ to a frame of axes rotating at a rate $\Omega(t) = d\phi/dt$ about the 3-axis. In the new frame

$$\frac{d\vec{r}'}{dt} = \vec{\omega}' \times \vec{r}', \tag{32a}$$

$$\hbar\omega_1' = -\gamma A(t)$$
$$\omega_2' = 0, \tag{32b}$$

and

$$\omega_3' = \omega_0 - \Omega(t). \tag{32c}$$

The vector $\vec{r}$ for an atom in the lower (or upper) state has $r_3 = 1$ (or -1) and $r_1 = r_2 = 0$.

The response of the quantum system to the chirped pulse is represented by the precession of the state vector $\vec{r}'$ about the resultant $\vec{\omega}'$ while the latter vector is tipped slowly (compared to the precession rate) through 180°. This is depicted in Fig. 8 where $d\Omega/dt$ and A are positive and the system is resonant at that $\Omega(t)$ where A(t) is maximum. If $d\Omega/dt$ is constant, the curve of Fig. 8 has the same shape as the envelope A(t). The semivertical angle of the cone of precession is approximately equal to the angle through which $\vec{\omega}'$ turns in the time that $\vec{r}'$ takes to precess 90° about the initial $\vec{\omega}'$. This is given by the relation:

$$\delta\theta \approx \frac{\pi\gamma\left(\frac{dA}{dt}\right)_0}{2\hbar\left[\omega_0 - \Omega(0)\right]^2} + \frac{\pi^2\gamma\left(\frac{d^2A}{dt}\right)_0}{8\hbar\left[\omega_0 - \Omega(0)\right]^3}. \tag{33}$$

Here the zero denotes conditions at the beginning of the pulse. Because the envelope A(t) starts from zero and ends at zero, it is not necessary to sweep over a large range as in the corresponding NMR experiments where the rf field amplitude is kept constant.

The adiabatic condition (constant $\delta\theta$) is that the rate at which $\vec{\omega}'$ is tipped should be always small compared to the rate of precession of $\vec{r}'$ about $\vec{\omega}'$. Near the middle of the pulse this yields the relation

$$\gamma A_{max}/\hbar \gg \frac{\hbar\dot{\Omega}}{\gamma A_{max}} \tag{34a}$$

or

$$\dot{\Omega} \ll \left(\frac{\gamma A_{max}}{\hbar}\right)^2. \tag{34b}$$

Near the ends of the pulse the same condition yields

$$\frac{\Delta\Omega}{2} \gg \frac{2\gamma\left(\frac{dA}{dt}\right)_{max}}{\hbar\,\Delta\Omega} \tag{35a}$$

or

$$\left(\frac{dA}{dt}\right)_{max} << \frac{\hbar(\Delta\Omega)^2}{4\gamma} \qquad (35b)$$

An additional condition is that the pulse length ought to be short compared to the time between dephasing collisions.

The vector $\vec{r}'$ will follow either $\vec{\omega}'$ or $-\vec{\omega}'$, depending on whether the two vectors are initially parallel or antiparallel. The induced polarization is proportional to the component r_1, while the field is opposite to ω_1; so that the induced polarization will be in the same direction as the driving field if the frequency sweep is negative and the system is initially in its ground state. This will produce a decrease in pulse propagation speed. Reversing the sweep direction (or the population difference) produces a polarization 180° out of phase with the E-field, and this will have some effect (perhaps defocusing) on the stability of the propagating pulse.

For the experimental attempt to observe these effects, we have built a CO_2 laser for generating optical chirps of 10.6 microns wavelength, 0.5 to 1.0 microsecond pulse duration and 60 MHz sweep, and will use this laser as a source for inverting the ν_3 vibration of sulphur hexafluoride (SF_6) between the ground and first excited states. Except for the chirp feature, the laser is of fairly standard design: water-cooled, external flat and spherical mirrors, sodium chloride Brewster windows, aperture stops for selection of dominant mode (TEM_{00n}). The laser configuration is shown in Fig. 9.

The frequency is swept by changing the optical cavity length. This is accomplished mechanically by rotating the flat mirror by a synchronous 1800 rpm motor with an offset of a centimeter or two between the rotation axis and the laser axis. The cavity length of 150 cm provides a spacing of 100 Mc for the TEM_{00n} modes while the CO_2 line width is about 60 Mc. Figure 10 shows a set of pulses generated by this scheme. The 2 μsec spacing between the pulses corresponds to an offset of about 1.3 cm of the rotating mirror. The biggest pulse in the train occurs when the laser mode is on axis with the aperture stops.

The frequency sweep is produced by the motion of the mirror, which gives a time-dependence to the optical cavity frequency ν_c. When the laser pulse begins, its frequency is given by

$$\nu = \left(\nu_c(1) + \frac{Q_L}{Q_c}\nu_L\right)/(1+Q_L/Q_c) \qquad (36)$$

where subscripts C and L refer to the optical cavity and the CO_2 line, respectively, and Q is the quality factor of the respective resonance. Thereafter, the stimulated emission is in phase with the stimulating radiation, the frequency of which is being swept continuously as a result of the almost adiabatic change in mode volume produced

by the moving mirror. During the whole pulse, the frequency probably remains governed by the formula above. Therefore, it is essential to have $Q_L/Q_C << 1$. For our cavity, which has a length of 150 cm and power coupling η equal to 0.21 (due to a sodium chloride flat tilted for 20° angle of incidence), we estimate that Q_C is about 8.6×10^6 (neglecting internal losses). Assuming a 60 Mc line width for CO_2, we have a Q_L of about 5×10^5, so that

$$Q_L/Q_C \doteq 0.06. \tag{37}$$

We have observed a frequency sweep of about 60 Mc in our pulses. Using a Michelson interferometer arrangement with a path length difference of 35 meters, we beat the pulse against itself and observed a 7 Mc signal. The results are shown in Fig. 11, which shows the detector response to the pulse (a) from one arm of the Michelson interferometer and (b) from both simultaneously. This technique will be developed further.

The experiments on SF_6 will be of two kinds, viz., the response of the SF_6 medium to the optical chirps, and the effect of the medium on the pulse propagation. Patel and Slusher (Ref. 24) have used the coincidence of the SF_6 and CO_2 lines to study self-induced transparency. It is probable that the CO_2 line lies in one Doppler wing of the SF_6 absorption and that the SF_6 matrix element is much larger than the reported value (Ref. 24) of 3×10^{-20} esu. The pulse will then select for inversion those SF_6 molecules that fall into a certain velocity component range.

We do not expect to observe self-induced transparency, because of the frequency sweep in our pulses. We hope to observe stimulated emission from the SF_6 following its inversion, and we aim to look for asymmetries in the pulse propagation speed and self-focusing or defocusing effects with respect to the magnitude and sign of the frequency sweep. The Michelson interferometer scheme may be useful in measuring time delay and phase distortion of the propagating pulse. Focusing and defocusing effects will be studied by observation of diffraction patterns.

MEASUREMENT OF NANOSECOND FLUORESCENCE DECAY TIMES

The simplest type of lifetime determination is the measurement of a fluorescence decay time. Since the early 1930's it has been possible to measure fluorescence lifetimes as short as one nanosecond (Ref. 25). However, the fluorometers devised for these measurements are complex and cumbersome. Moreover, insomuch as the actual decay curve is not observed, the measurements are indirect. This latter deficiency leads to serious problems of competing channels of decay are in evidence. Therefore, a simpler and more direct technique for measuring rapid fluorescence decay rates is desirable.

To observe a fluorescent decay, a high-intensity source having a rapid fall time is required to excite the fluorescence and a wide bandwidth detection system is needed to detect it. Mode-locked lasers are an ideal excitation source. A

number of different lasers have been successfully mode-locked. Of these, the simultaneously Q-switched and mode-locked ruby (Ref. 26) or neodymium (Ref. 7) lasers offer the greatest peak output power. For materials absorbing in the blue end of the spectrum rather than in the red, frequency doubling may be employed with these lasers. In addition to the pulsed phase-locked lasers, the argon laser (Ref. 27) and the Nd^{+3}:YAG laser (Ref. 28) have been continuously mode-locked with appreciable peak output power. In all of the above lasers, the widths of the output pulses are considerably less than one nanosecond.

With the continuously mode-locked lasers, a crossed-field photomultiplier (Ref. 29) used in conjunction with a sampling oscilloscope could give an overall detection risetime as short as 0.06 nanosecond. Such a system could equal even the fastest modern fluorometer (Ref. 30). With the pulsed mode-locked lasers, a traveling wave oscilloscope must be used. These typically have a risetime of on the order of a few tenths of a nanosecond.

In the present case a simultaneously Q-switched and mode-locked ruby laser was used to excite the fluorescence. A UAC 1240 Phototransducer having a 0.3 ns risetime was used to detect the fluorescence radiation. The output from this detector was displayed on a Tektronix 519 oscilloscope. Figure 12a shows an oscilloscope tracing of the laser output. The pulse widths shown illustrate the time response of the detection system.

Two classes of dyes were investigated in this experiment, those excited directly by the ruby laser and those excited by the second harmonic of ruby. The former were the dyes commonly used for Q-switching the ruby laser, while the latter dyes were, for the most part, liquid laser dyes (Refs. 1, 31). The experimental arrangement used for the liquid laser dyes is shown in Fig. 13. A copper sulfate solution was used to absorb the scattered laser light, while a sharp cut interference filter was used to block the scattered second harmonic light. In that way only the fluorescence was detected by the photodiode. In all cases the concentrations of the dyes were adjusted to give a transmission through the 1-cm dye cell of approximately 10% at 3470 Å.

A typical oscilloscope tracing of a fluorescence is shown in Fig. 12b. The decay times for the various dyes were determined by fitting an exponential to each of the decaying portions in the oscillographs. For each dye the results from two such photographs (i.e., ten curves) were then averaged together. The results for the liquid laser dyes are summarized in Table I. The values given for the lifetimes should be accurate to better than ± 20%.

The setup used for determining the fluorescence lifetime of the Q-switching dyes was quite similar to that used for the liquid laser dyes. Of course, since the Q-switching dyes are excited directly by the laser beam, frequency doubling was not necessary. To detect the fluorescence, an S-1 version of the UAC 1240 photodiode was used. A Corning Glass Works CS-7-69 filter was used to separate the scattered laser light from the fluorescence.

Three Q-switching dyes were investigated, chloro-aluminum phthalocyanine, vanadyl phthalocyanine, and cryptocyanine. In the case of the phthalocyanines, the lifetimes were measured in several solvents. The concentrations were adjusted for a transmission of about 10% at 6943 Å through the 1-cm-thick dye cell. In the case of chloro-aluminum phthalocyanine in ethanol, the concentration was varied to give a transmission of from 4% to 75% to determine if the lifetime depended on concentration. No such dependence was found. The results are summarized in Table II.

The fluorescent decay in cryptocyanine was by far the most rapid. The measurement there was limited by the detection system response time. Spaeth and Sooy (Ref. 32) have estimated a decay time of 4×10^{-11} seconds for cryptocyanine in propanol. It is quite possible that the fluorescence decay time in a methanol solution is as short. The lifetime measured for chloro-aluminum phthalocyanine in 1-chloronaphthalene is somewhat longer than reported by Bowe, et al (Ref. 33) though the difference is only 0.1 ns outside of the experimental errors. The result for vanadyl phthalocyanine in nitrobenzene is in good agreement with that obtained by Arecchi, et al (Ref. 34).

LIGHT AMPLIFICATION IN SATURABLE ABSORBERS (LAISA) WITH PICOSECOND PULSES

Fluorescence measurements are limited by the risetime of the electronics involved. This difficulty can be circumvented in materials exhibiting a saturable absorption at the laser wavelength. An experimental arrangement which was set up for measuring the recovery time in such absorbers is shown in Fig. 14. The laser beam impinges on a dye cell which is canted by a slight angle, θ, as illustrated in Fig. 14. Most of the beam passes through the dye cell but a small amount is reflected by it. The reflected beam strikes an inclined wedge and part of this beam is reflected back onto itself by the surface of the wedge as shown. The net [illegible] is that two beams pass through the dye: the first, an intense beam, and the [illegible] beam inclined to the first by an angle 2θ and delayed in time [illegible] approximately $\frac{2S}{c}$ where S is the spacing between the [illegible] The use of wedges avoids

The shortest recovery time which could be measured in this experiment would be approximately the duration of the mode-locked pulses themselves. The pulse duration for the ruby laser used in this experiment was measured using a double quantum absorption-fluorescence technique (Ref. 35) and was found to be approximately 2×10^{-11} seconds. This is considerably better than could be hoped for in a fluorescence measurement.

The first dye studied was cryptocyanine in methanol. Its decay time was found to be shorter than 0.5 ns in the fluorescence measurements. The output of the photodiode when the cell is filled with methanol is shown in Fig. 15a. The first of the two pulse trains is the incident pulse, while the second is the transmitted and delayed pulse. The amplitudes are about equal and remain equal irrespective of the delay (i.e., that due to the spacing between the dye cell and the wedge). Cryptocyanine was then added to the methanol in the dye cell to give a solution with an optical density of approximately 5.0 at 6943 Å. With a 2.0 picosecond delay, the results are shown in Figs. 15b and 15c.

The striking feature in Figs. 15b and 15c is that early in the pulse trains the delayed signal is amplified rather than attenuated. Furthermore, if the transmission of the primary (undelayed) beam through the dye cell is monitored simultaneously with the transmission of the delayed beam, it is found that when the delayed beam is amplified more greatly, the primary beam is attenuated more strongly. This, plus several other experiments, indicates that the effect is a real one and that it is due to some hitherto unnoticed feature of the dye. It is suggested that such devices be called LAISA for "Light Amplification in Saturable Absorbers."

Because this phenomenon prevents the measurement of saturable absorber recovery time, the recovery time experiments were temporarily halted in favor of experimentation to discover the nature of the nonlinear amplification effect. It was hoped that with an understanding of the phenomenon it might be possible to eliminate the gain effect and repeat the lifetime experiments in the future. In addition, the amplification is interesting and important in itself.

One of the first experiments performed to explore the nature of the nonlinear effect simply involved taking far field photographs of the beams passing through the dye cell. A one-meter focal length camera was used for this purpose. Figure 16a shows the result when the cell is filled with just methanol. The weaker of the two spots is the delayed beam. Here, again, the delay was 2 picoseconds. The dye cell was then filled with a cryptocyanine in methanol solution (O.D. 1.0 at 2943 Å) and the far field pattern was retaken. The result is displayed in Fig. 5b. [illegible] the delayed beam is apparent from this photograph. More important, [illegible] of the weaker beam on the opposite side of the primary [illegible] 14 that such a beam cannot be produced by a [illegible] f this beam in the dye is highly suggestive of [illegible]

Further evidence of a parametric process was obtained both photographically and photoelectrically by noting the variation of gain in the delayed beam as a function of the delay time. It was found that there is gain only when there is an appreciable overlap of the pulses in the delayed beam with those in the primary beam. That is to say, there is gain only when the delay is comparable to or less than the pulse duration (20 picoseconds).

With a parametric process there is the possibility of a frequency shift. This was investigated next. This was done by placing a transmission grating after the dye cell and by repeating the previous photographs in the first order spectrum. The results are shown in Figs. 17 and 18. The angular shift between the delayed and undelayed beams is displayed in the horizontal direction, while frequency spread is displayed in the vertical direction. The dispersion in the vertical direction is approximately 12 Å/mm. It should be noted that the angular divergence of the laser beam also contributes to the size of the spots on the film and limits the resolution to perhaps 20 to 30 Å. It is clear from the photographs that if there is any frequency shift it is less than the 20 or 30 Å resolution limit.

Figures 17 and 18 also show the dependence of the gain phenomenon on the angular displacement between the delayed and undelayed beams. At large angles the delayed beam is amplified but there is no generation of the third beam. As the angle is reduced, the third beam grows in prominence until it is nearly as intense as the amplified delayed beam. In addition, one or more secondary beams also appear. Finally, at very small angles there appears to be a loss of gain for the delayed beam and for the third beam.

In the last experiment performed to date, a number of saturable absorbers were examined to see if any differences in the gain effect occurred. All of the saturable polymethine cyanine dyes, cryptocyanine, dicyanine A and 1, 1'-diethyl-2, 2'-dicarbocyanine iodide, were tried as was chloroaluminum phthalocyanine. The polymethine cyanines were each tried in three solvents: methanol, acetone and dimethyl sulfoxide. Despite the differences in the peak absorptions in the different polymethines and despite the widely different solvent shifts for the three solvents, all the dye-solvent combinations showed the effect to about the same degree. The effect was equally pronounced in chloroaluminum phthalocyanine in ethanol. The gain phenomenon is, therefore, common to all the saturable absorbers normally used with ruby lasers.

The universality of the gain effect in saturable absorbers suggests that the effect is intimately connected with the saturable absorption itself. Indeed, a qualitative description of the process can be devised assuming only that the absorption of the dye solution decreases with increasing incident intensity. Consider the case of two plane monochromatic waves, one of much lower intensity than the other and of slightly different frequency, incident upon the medium. Because of the slight difference in frequency, the intensity within the medium is modulated at the beat frequency of the two waves. The degree of modulation in the transmitted beam is enhanced over that in the incident beam because of the nonlinear absorption

in the medium. This is equivalent to saying that the weaker beam is amplified. The degree of amplification is dependent on the slope of the attenuation vs intensity curve for the dye solution at the intensity being used. Because the modulation in the transmitted beam is no longer sinusoidal, the process also results in the generation of harmonics. In the event that the two incident beams are not collinear, the various frequency harmonics will be generated in different directions.

The process can also be viewed as a nonlinear change in the index of refraction which is brought about by the saturation of the absorption line. The case where the refractive index change is proportional to the incident intensity as it is, for example, in Kerr active liquids, has been treated by Chiao, Kelly and Garmire (Ref. 36). Again one finds that the weaker beam is amplified and that frequency harmonics are generated. It is worth noting that the salient features of the angular dependence predicted by Chiao, et al for the gain of the weak beam and for the most important harmonic are in accord with the present observations.

Although the gain process is fairly well understood qualitatively, more work must be done to obtain a quantitative understanding of the effect. One complication to the problem is that practical saturable absorbers are not simple two-level systems (Ref. 37). In fact, the loss of gain in the rear portion of the pulse trains (see Fig. 15) is very likely due to the transfer of population from the saturably absorbing singlet manifolds to the lowest triplet manifold.

Since the saturable absorbing dyes are an integral part of many ruby laser systems, this nonlinear effect is an important one. One obvious result is the enhancement of the gain in the off-axis modes of the laser cavity. If an appreciable amount of power is coupled into these modes, a degradation of beam collimation would be experienced. In the mode-locked laser, nonaxial propagation would also result in a broadening of the individual pulses and possibly in a multiplicity of pulse trains.

A Galilean telescope is incorporated in the mode-locked ruby laser used for these experiments. This telescope doubles the beam diameter just before the beam passes through the saturable dye and strikes the 100% reflecting mirror. The telescope was added to the cavity in order to eliminate the deterioration of the 100% mirror. However, it was also found to improve the beam divergence substantially and to improve the quality of the pulse trains. It is possible that some of this improvement is the result of the reduced intensity at the dye cell.

SIX-MONTH STATUS EVALUATION

The theoretical and experimental research performed by the Research Laboratories of United Aircraft Corporation during the six-month interval from 1 August 1967 to 31 January 1968 on the subject contract has resulted in the following enhancement of the state of the art of the ultrashort laser pulse technology field:

(a) Mode-Locking of an Organic Dye Laser. This accomplishment should make available picosecond optical pulses throughout the visible portion of the spectrum. The availability of ultrashort pulses at any desired wavelength would greatly increase their applicability to studies of nonlinear optical effects, spectroscopy, lifetime measurements, etc.

(b) Optical Rectification of Mode-Locked Laser Pulses at Microwave Frequencies. This accomplishment opens up the possiblity of generating millimeter or submillimeter waves with ultrashort optical pulses and obtaining a detector for picosecond pulses because of the broad band response of the optical rectification effect. The detection of optical rectification at approximately 10 GHz has eliminated spurious signals from pyroelectric and acoustic effects, therefore simplifying the detection of this effect. The use of simultaneously Q-switched and mode-locked pulses enables the use of the high sensitivity characteristics of radio receivers in many experiments where signal sensitivity may be a problem.

(c) Analytical Solution for 2π and 4π Optical Pulses. This accomplishment should lead to a better understanding of the transient response of quantum systems.

(d) Theoretical Prediction of Adiabatic Inversion of Quantum States. This accomplishment should result in a better understanding of the transient response of quantum systems when subjected to a frequency-swept laser pulse.

(e) 60 MHz Frequency-Swept, Q-Switched CO_2 Laser Pulse. This accomplishment should open up new experimental possibilities in studying transient response of quantum systems and in optical ranging, radar, signal processing, etc.

(f) Measurement of Nanosecond Fluorescence Decay Times. This accomplishment has demonstrated the ease at which subnanosecond fluorescence lifetime can be measured with ultrashort laser pulses having peak powers of the order of gigawatts. This technique should therefore be of great help to spectroscopists in their study of solids, liquids, and gases.

(g) Light Amp..ification in Saturable Absorbers (LAISA) with Picosecond Pulses. This accomplishment has resulted in a new method for amplifying light waves and therefore suggests that the device be called as "LAISA", an acronym for "Light Amplification in Saturable Absorbers."

REFERENCES

1. Sorokin, P. P., J. R. Lankard, E. C. Hammond and V. L. Morruzi: IBM Journal, 11, 130 (1967).

2. Bass, M. and T. F. Deutsch: Appl. Phys. Letters 11, 89 (1967).

3. Soffer, B. H. and B. B. McFarland: Appl. Phys. Letters 10, 266 (1967).

4. Spaeth, M. L. and D. P. Bortfeld: Appl. Phys. Letters 9, 179 (1966).

5. Schaffer, F. P., W. Schmidt, Jurgen Volze: Appl. Phys. Letters 8, 306 (1966).

6. DeMaria, A. J., D. A. Stetser and W. H. Glenn, Jr.: Science 156, 1557 (1967).

7. DeMaria, A. J., D. A. Stetser and H. A. Heynau: Appl. Phys. Letters 8, 174 (1966).

8. Bass, M., P. A. Franken, J. F. Ward and G. Weinreich: Phys. Rev. Letters 9, 446 (1962).

9. Brienza, M. J. and A. J. DeMaria: Appl. Phys. Letters 11, 44 (1967).

10. Glenn, W. H., Jr. and M. J. Brienza: Appl. Phys. Letters 10, 221 (1967).

11. Armstrong, J. A.: Appl. Phys. Letters 10, 16 (1967).

12. Giordmaine, J. A., P. M. Rentzepis, S. L. Shapiro and K. W. Wecht: Appl. Phys. Letters 11, 216 (1967).

13. Stetser, D. A. and A. J. DeMaria: Appl. Phys. Letters 9, 118 (1966).

14. McCall, S. L. and E. L. Hahn: Phys. Rev. Letters 18, 908 (1967).

15. Patel, C. K. N. and R. E. Slusher: Phys. Rev. Letters 19, 1019 (1967).

16. Basov, N. G., R. V. Ambartsumyan, V. S. Zuev, P. G. Kryukov and V. S. Letakhov: Soviet Physics, JETP 23, 16 (1966).

17. Seeger, A., H. Douth and A. Kochendoerfer: Z. Physik 134, 173 (1953).

18. Lamb, G. L., Jr.: Physics Letters 25A, 181 (1967).

19. Abragam, A.: The Principles of Nuclear Magnetism. Oxford University Press, 1961.

20. Abella, I. D., S. R. Hartmann and N. A. Kurnit: Physical Review 141, 391 (1966).

REFERENCES
(cont'd)

21. Hahn, E.: Phys. Rev. 80, 580 (1950).

22. Carr, H. Y. and E. M. Purcell: Phys. Rev. 94, 630 (1954).

23. Feynman, R. P., F. L. Vernon and R. W. Hellwarth: J. Appl. Phys. 28, 49 (1957).

24. Patel, C. K. N. and R. E. Slusher: Phys. Rev. Letters 19, 1019 (1967).

25. Szymanowski, W., Z. f. Phys. 95, 450 (1935); P. Pringsheim, Fluorescence and Phosphorescence, pp. 10-17, Interscience Publishers, New York, 1949.

26. Mocker, H. W. and R. J. Collins: Appl. Phys. Letters 7, 270 (1965).

27. Crowell, M. H.: IEEE (Inst. Elec. Electron. Engrs.) J. Quantum Electron 1, 12 (1965).

28. DiDomenico, M., J. E. Geusic, H. M. Marcos and R. G. Smith: Appl. Phys. Letters 8, 180 (1966).

29. Fisher, M. B. and R. T. McKenzie: International Electron Devices Meeting, Washington, D. C., October 1967.

30. Carbone, R. J. and P. R. Longaker: Appl. Phys. Letters 4, 32 (1964).

31. Sorokin, P. P. and J. R. Lankard: IBM Journal 11, 148 (1967).

32. Spaeth, M. L. and W. R. Sooy: 4th International Conference on Quantum Electronics, 1966.

33. Bowe, P. W. A., W. E. K. Gibbs and J. Tregellas-Williams: Nature 209, 65 (1966).

34. Arecchi, F. T., V. Degiorgio and A. Sona: Nuovo Cimento 38, 1096 (1965).

35. Glenn, W. H., A. J. DeMaria and M. J. Brienza: Quarterly Research Report

36. Chiao, R. Y., P. Kelley, E. Garmire: Phys. Rev. Letters 17, 1158 (1966).

37. Giuliano, C. R. and L. D. Hess: J. Quantum Electronics 3, 358 (1967).

TABLE I - LIQUID LASER DYES

DYE	SOLVENT	FLUORESCENT PEAK	FLUORESCENT LIFETIME
Acridine Red	Ethanol	5800Å	2.4 nsec
Acridine Yellow	Ethanol	5050Å	5.2 nsec
Sodium Fluorescein	Ethanol	5270Å	6.8 nsec
Rhodamine 6G	Ethanol	5550Å	5.5 nsec
Rhodamine 6G	Water	5550Å	5.5 nsec
Acridone	Ethanol	4370Å	11.5 nsec
Anthracene	Methanol	4000Å	4.5 nsec

TABLE II - Q-SWITCHING DYES

DYE	SOLVENT	ABSORPTION PEAK	FLUORESCENCE PEAK	LIFETIME
CAP	Ethanol	6700Å	7750Å	10.1 nsec
CAP	Methanol	6710Å	7550Å	10.3 nsec
CAP	Chloronaphthalene	6970Å	7380Å	8.0 nsec
VP	Nitrobenzene	6980Å	--	4.1 nsec
VP	Chloronaphthalene	7010Å	--	4.2 nsec
CC	Methanol	7060Å	7400Å	0.5 nsec

CAP = Chloro-Aluminum Phthalocyanine

VP = Vanadyl Phthalocyanine

CC = Cryptocyanine

LIST OF FIGURES

EXPERIMENTAL ARRANGEMENT FOR MODE-LOCKING OF AN ORGANIC DYE LASER

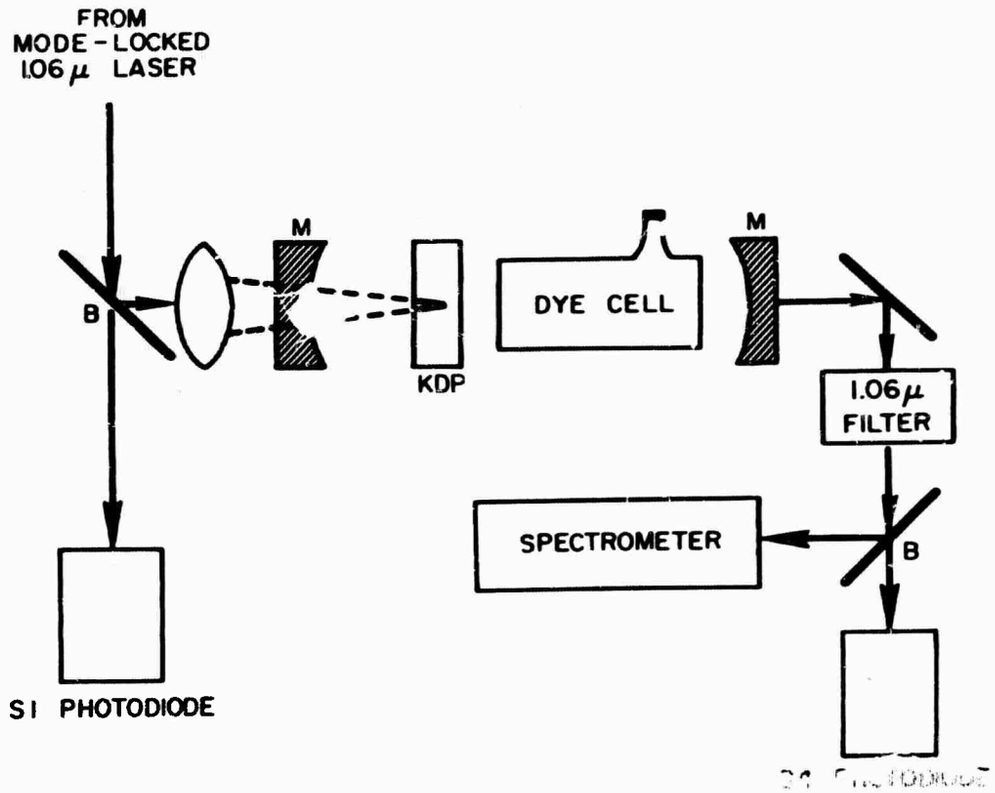

OSCILLOGRAMS AND SPECTRA OF A MODE-LOCKED DYE LASER

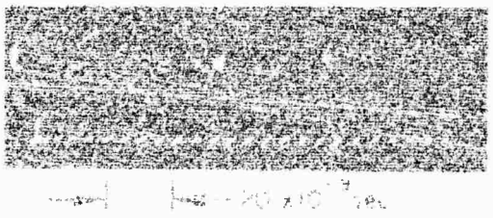

(a.) PUMPING PULSE TRAIN INPUT

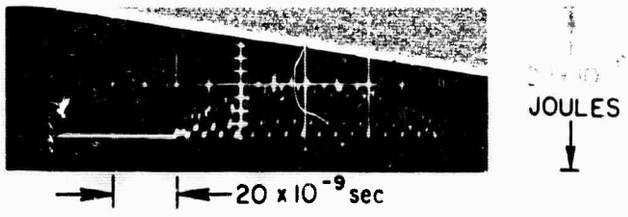

(b.) DYE LASER OUTPUT

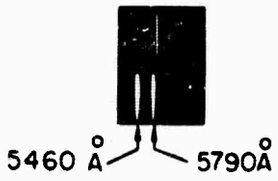

(c.) SPECTRUM OF RHODAMINE B LASER

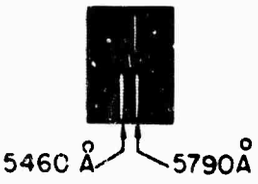

(d.) SPECTRUM OF RHODAMIME 6G AND B MIXTURE

ORIENTATION OF KDP CRYSTAL TO POLARIZATION OF REPETITIVE PULSE

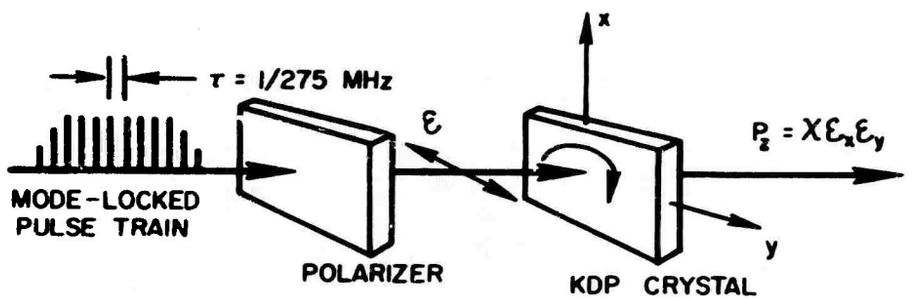

FIG. 3

FIG. 4

OPTICAL RECTIFICATION SIGNALS AT 2.75 GHz
AS A FUNCTION OF CRYSTAL ORIENTATION

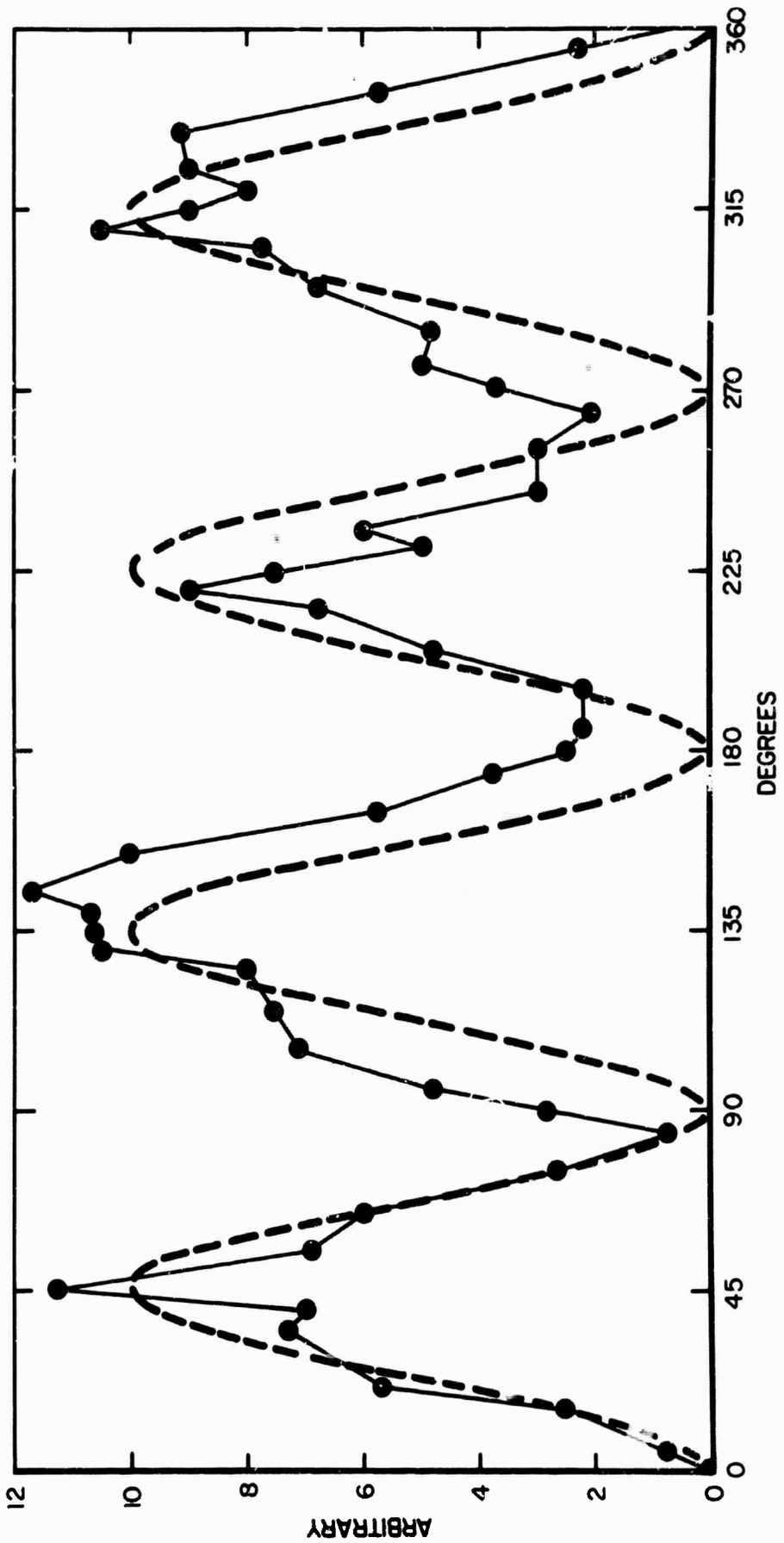

FIG. 5

OPTICAL RECTIFICATION

RECEIVER OUTPUT

LASER OUTPUT

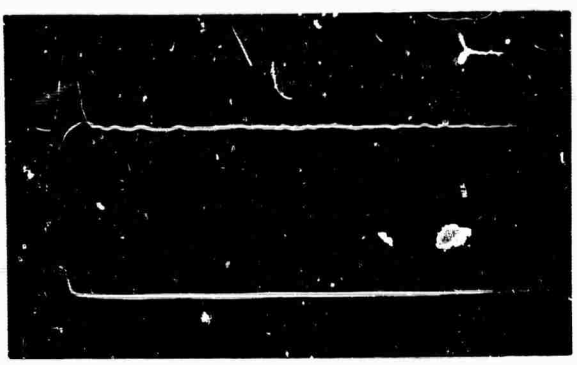

SWEEP SPEED:
0.5 μsec/div

6th HARMONIC - 650 MHz

LASER OUTPUT

SWEEP SPEED:
100 nsec/div

FIG. 6

PROPAGATION OF A 4π PULSE IN AN ABSORBING MEDIUM

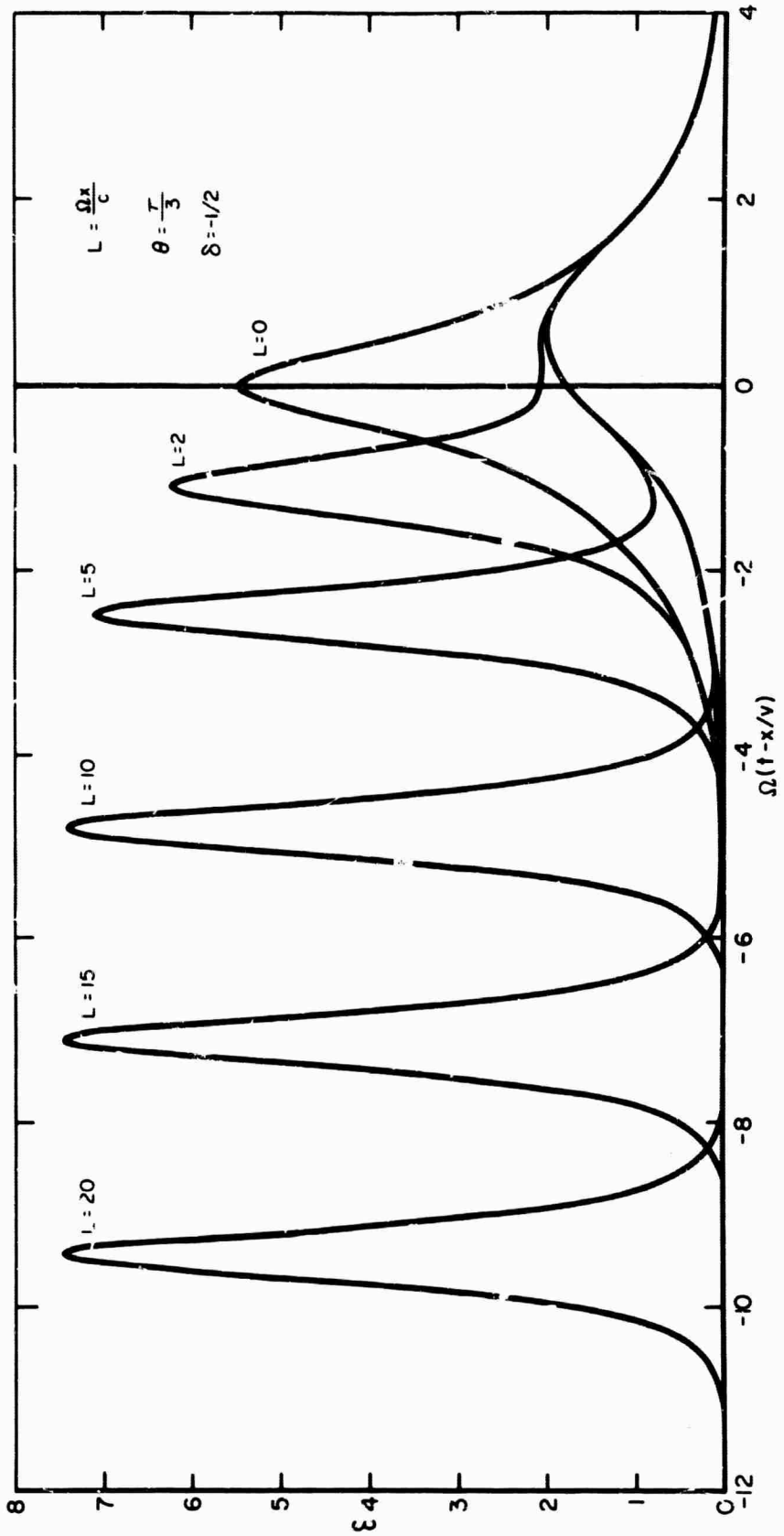

FIG. 7

PROPAGATION OF A 4π PULSE IN AN ABSORBING MEDIUM

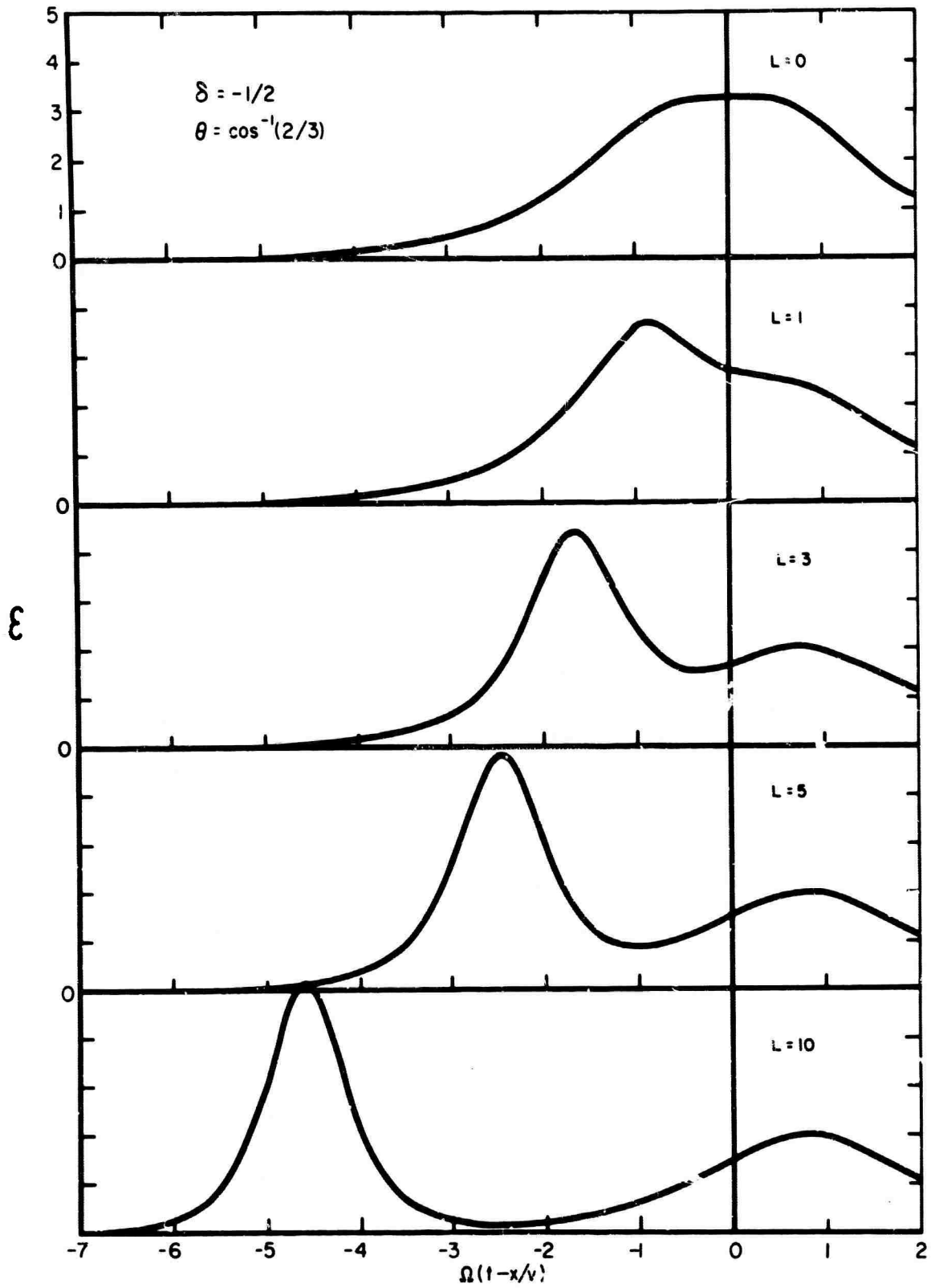

GEOMETRICAL REPRESENTATION OF ADIABATIC INVERSION

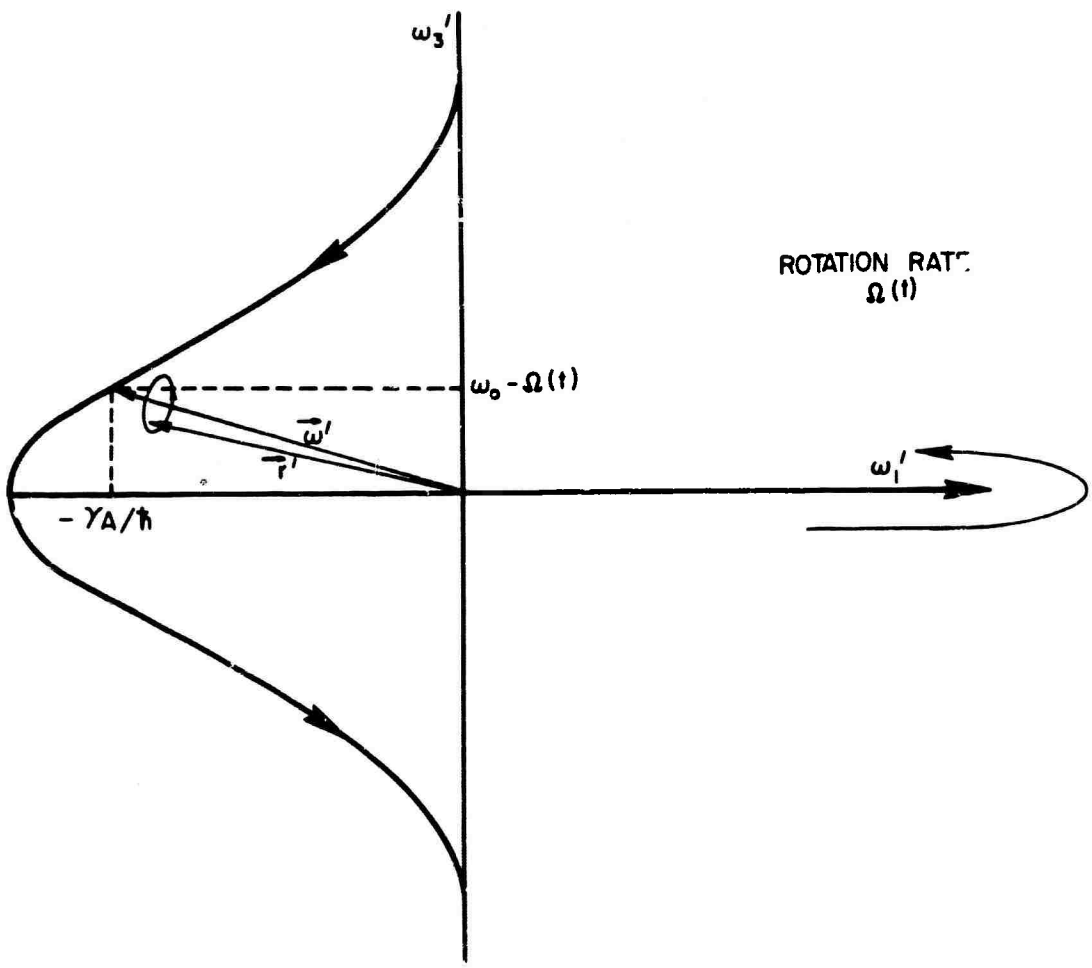

FIG. 9

LASER CONFIGURATION FOR GENERATING FREQUENCY-SWEPT PULSES

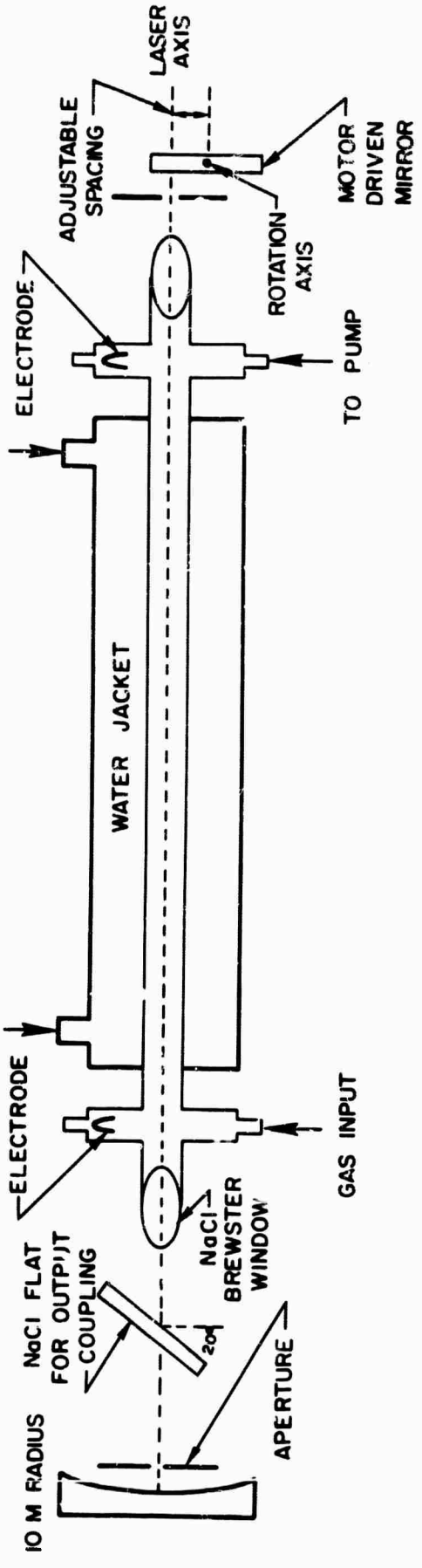

FIG. 10

TYPICAL OSCILLOGRAMS OF CHIRPED Q-SWITCHED CO_2 PULSES

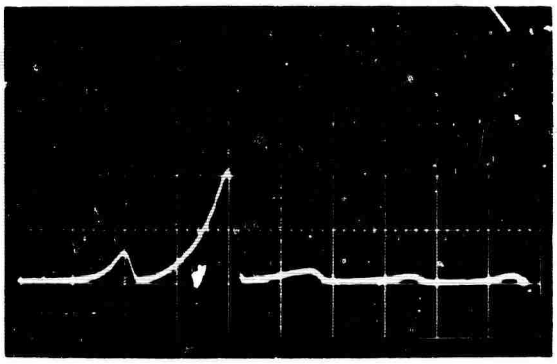

FIG. 11

EXPERIMENTAL EVIDENCE OF A CHIRPED Q-SWITCHED CO_2 LASER PULSE

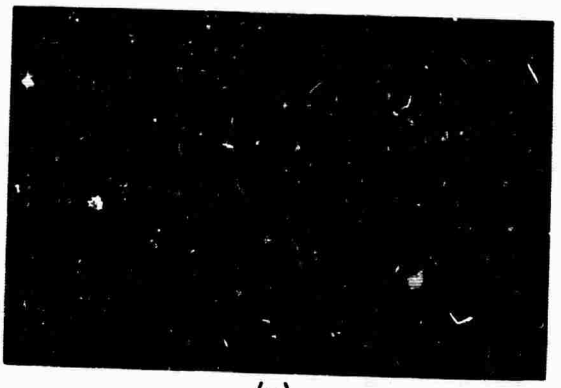

(a)

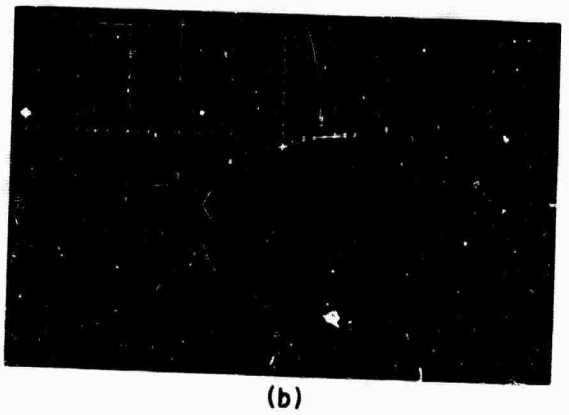

(b)

F-920479-6

FIG. 12

TYPICAL OSCILLOGRAMS

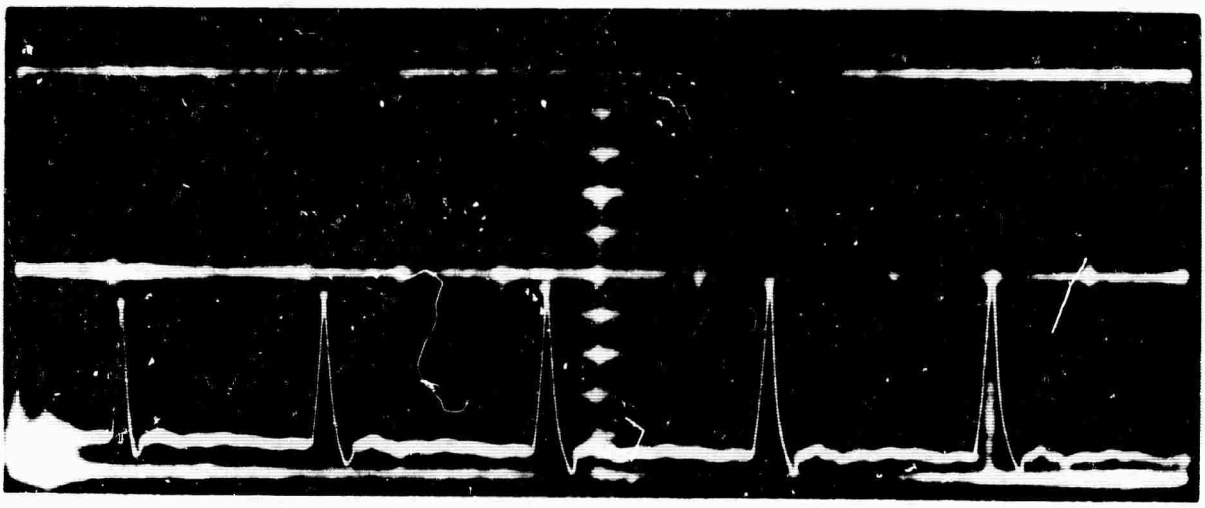

(a) MODE - LOCKED RUBY LASER OUTPUT - 10 nsec/cm

(b) FLUORESCENCE DECAY TIME OF FLUORESCEIN SODIUM - 10 nsec/cm

FIG. 13

EXPERIMENTAL ARRANGEMENT USED FOR LIQUID LASER DYE LIFETIME MEASUREMENTS

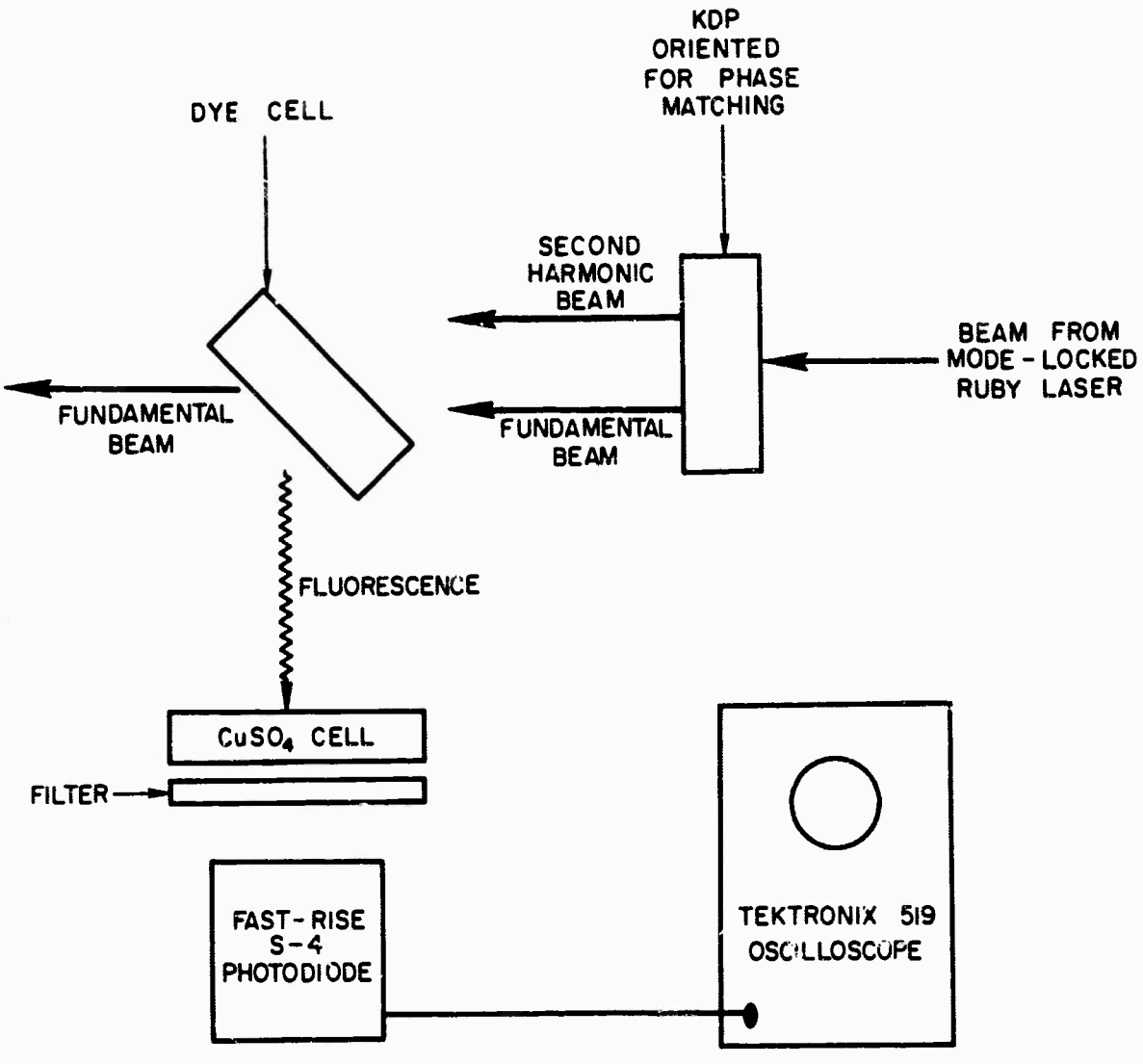

FIG. 14

EXPERIMENTAL ARRANGEMENT FOR MEASURING RECOVERY TIME IN SATURABLE ABSORBERS

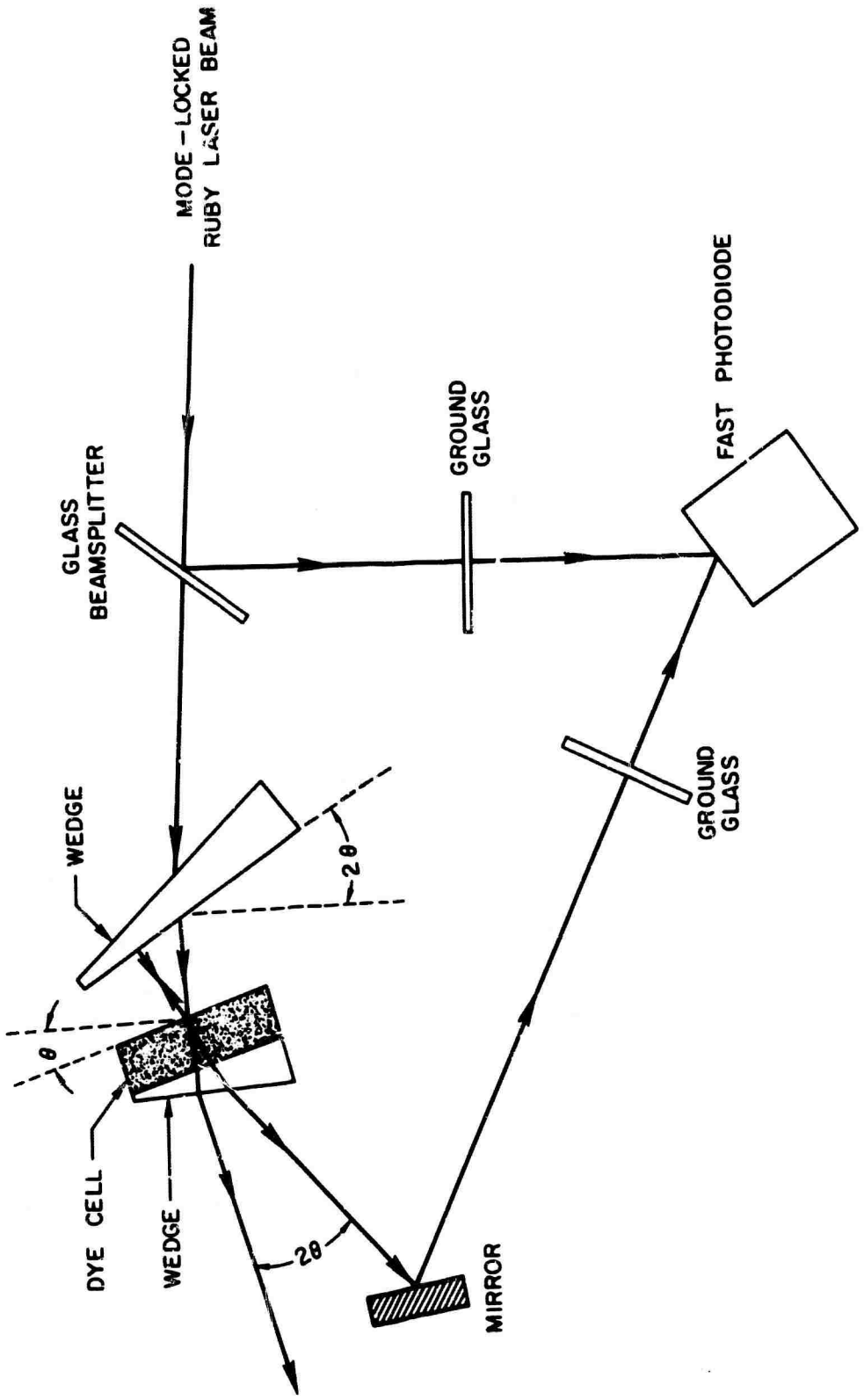

FIG. 15

SATURABLE ABSORBER RECOVERY EXPERIMENT

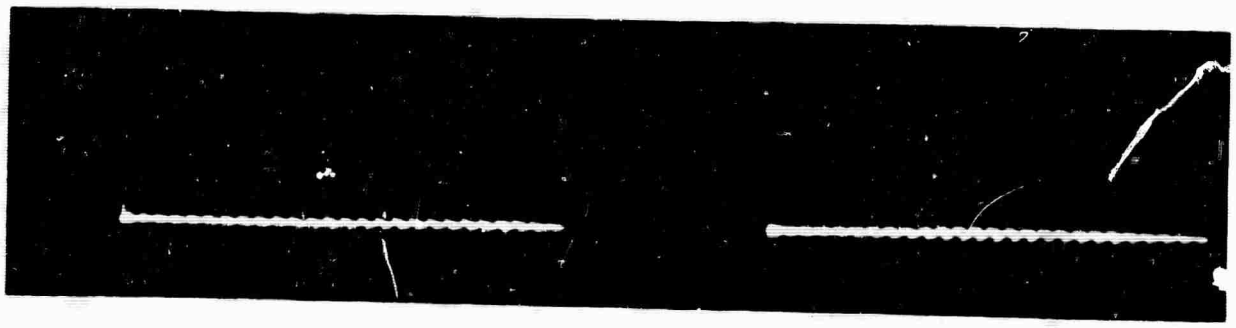

(a) METHANOL ONLY

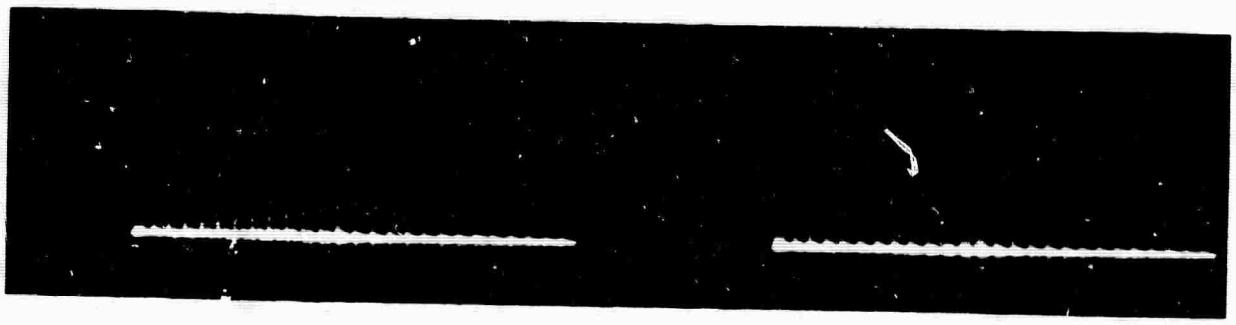

(b) METHANOL PLUS CRYPTOCYANINE

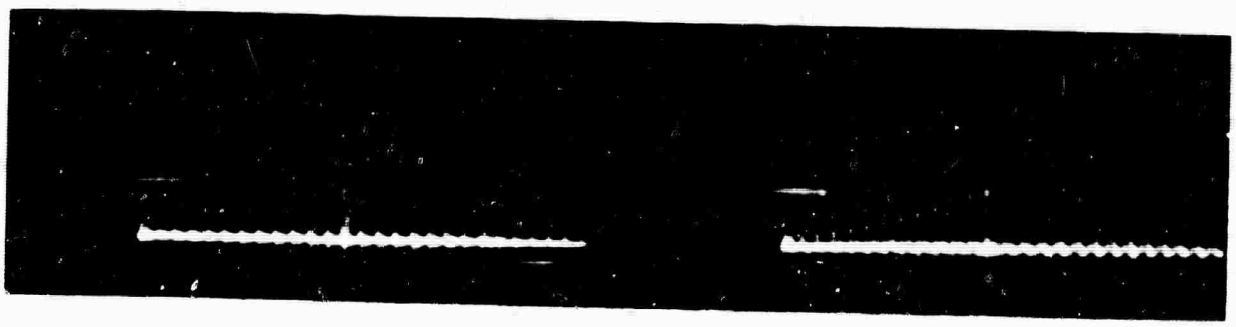

(c) METHANOL PLUS CRYPTOCYANINE

PARAMETRIC GENERATION IN CRYPTOCYANINE

(a)

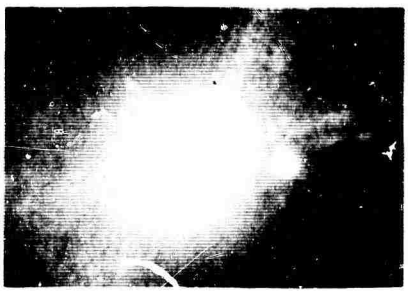

METHANOL ONLY

(b)

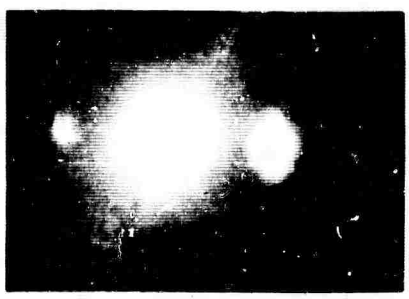

METHANOL PLUS CRYPTOCYANINE

FIG 17

ANGULAR AND FREQUENCY DEPENDENCE IN THE PARAMETRIC EFFECT

(a) θ = 32 MRAD

(b) θ = 25 MRAD

(c) θ = 11 MRAD

ANGULAR AND FREQUENCY DEPENDENCE IN THE PARAMETRIC EFFECT

$\theta = 7$ MRAD
(a)

$\theta = 4$ MRAD
(b)

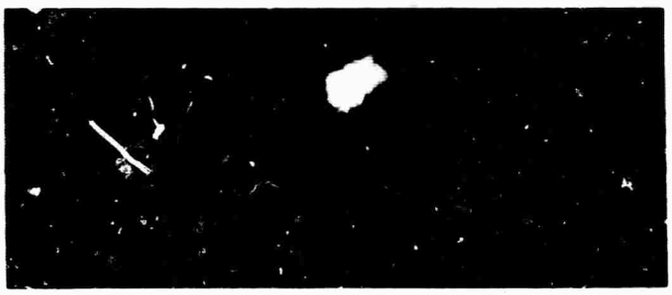

$\theta = 2.5$ MRAD
(c)

BLANK PAGE

Unclassified
Security Classification

DOCUMENT CONTROL DATA - R & D

(Security classification of title, body of abstract and indexing annotation must be entered when the overall report is classified)

1. ORIGINATING ACTIVITY (Corporate author)	2a. REPORT SECURITY CLASSIFICATION
United Aircraft Corporation Research Laboratories East Hartford, Connecticut	Unclassified 2b. GROUP

3. REPORT TITLE

Semiannual Report on the Research Investigation of Laser Line Profiles

4. DESCRIPTIVE NOTES (Type of report and inclusive dates)

Semiannual Report for the Period 1 August 1967 - 31 January 1968

5. AUTHOR(S) (First name, middle initial, last name)

A. J. DeMaria; M. J. Brienza; W. H. Glenn, Jr.; G. L. Lamb, Jr.; M. E. Mack; and E. B. Treacy

6. REPORT DATE	7a. TOTAL NO. OF PAGES	7b. NO. OF REFS
February 28, 1968	56	37

8a. CONTRACT OR GRANT NO.	9a. ORIGINATOR'S REPORT NUMBER(S)
N00014-66-C0344	F-920479-6
b. PROJECT NO.	
c.	9b. OTHER REPORT NO(S) (Any other numbers that may be assigned this report)
d.	

10. DISTRIBUTION STATEMENT

11. SUPPLEMENTARY NOTES	12. SPONSORING MILITARY ACTIVITY
	Department of the Navy Office of Naval Research

13. ABSTRACT

This report covers work performed under Contract N00014-66-C0344 for the period 1 August 1967 through 31 January 1968. Experimental results are presented on the mode-locking of an organic dye laser, the optical rectification of mode-locked laser pulses, the measurement of nanosecond fluorescent decay times, the observation of light amplification in saturable absorbers, and the generation of a 60 MHz frequency-swept, Q-switched CO_2 laser pulse. An analytical solution for 2π and 4π optical pulses and a theoretical prediction of adiabatic inversion of quantum states are presented.

DD FORM 1 NOV 65 1473

Unclassified
Security Classification

14. KEY WORDS	LINK A		LINK B		LINK C	
	ROLE	WT	ROLE	WT	ROLE	WT
Laser Line Profiles						